Journal of Energy Technology

JET Volume 13 (2020) p.p. 39-54
Issue 1, May 2020
Type of article 1.01
www.fe.um.si/en/jet.html

A SIMPLIFIED HYBRID METHODOLOGY FOR DESIGNING CORELESS AXIAL FLUX MACHINES

POENOSTAVLJENA METODA ZA NAČRTOVANJE SINHRONSKIH STROJEV S TRAJNIMI MAGNETI IN AKSIALNIM MAGNETNIM PRETOKOM BREZ FEROMAGNETNEGA JEDRA STATORJA

Franjo Pranjić[1,✉], Peter Virtič[1]

Keywords: Axial flux permanent magnet generator (AFPMG), approximation method, magnetic flux, magnetic flux density

Abstract

Axial flux permanent magnet generators (AFPMG) are used in many high torque applications, including wind generators. There are many design methodologies for AFPMG that are connected to simple design equations used for preliminary design. Analytical methods offer a fast preview of torque production of the designed machine with a certain degree of accuracy. The finite element method (FEM) is a more accurate numerical method than other methods and requires a great deal of time for simulations in the design procedure. This article presents a method for the design and analysis of an axial flux permanent magnet generator by using approximation polynomials.

✉ Corresponding author: Franjo Pranjić, Tel.: +386 3 777402, Mailing address: Koroška cesta 42a, E-mail address: franjo.pranjic@um.si

[1] University of Maribor, Faculty of Energy Technology, Hočevarjev trg 1, 8270 Krško

Povzetek

Sinhronskih generatorji s trajnimi magneti in aksialnim magnetnim pretokom (SGTMAMP) se uporabljajo v mnogih aplikacijah kjer so zahtevane visoke vrednosti navora, kot npr. za generatorje vetrnih elektrarn. Obstaja veliko metodologij za načrtovanje teh strojev, ki so povezane z analitičnimi enačbami za preliminarno načrtovanje tega tipa strojev.

Analitične metode ponujajo hiter predogled proizvodnje navora načrtovanega stroja z določeno stopnjo natančnosti. Numerične metode, in sicer metoda končnih elementov (MKE), so natančnejše od drugih metod in zahtevajo veliko časa za simulacije v postopku načrtovanja. V tem članku je predstavljena metoda za načrtovanje in analizo SGTMAMP z uporabo aproksimacijskega polinoma.

1 INTRODUCTION

Axial flux permanent magnet generators (AFPMG) have simple constructions, are compact, have a high degree of reliability and high-power density, *[1-7].* They are also called "disk-type" machines and have various topologies, depending on the application: single-sided (one stator and one rotor) shown in Fig.1; double-sided (single stator-double rotor or single rotor-double stator [6]) shown in Fig.2-Fig.4, and multi-stage (multiple rotors and stators) shown in Fig. 5 and Fig. 6, *[11,12].*

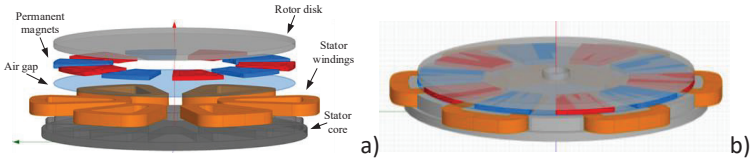

Figure 1: *Single-sided AFPMM: a) components of the machine, b) model of the machine*

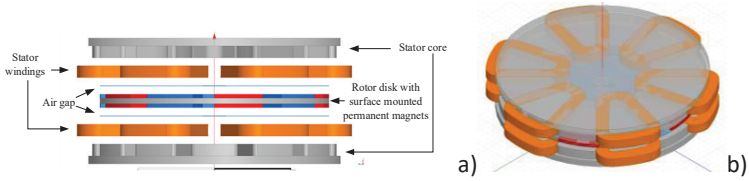

Figure 2: *Double-sided AFPMM with two external stators and one internal rotor: a) components of the machine, b) model of the machine*

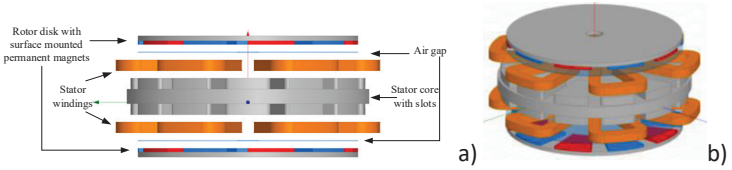

Figure 3: *Double-sided AFPMM with two external rotors and one internal stator: a) components of the machine, b) model of the machine*

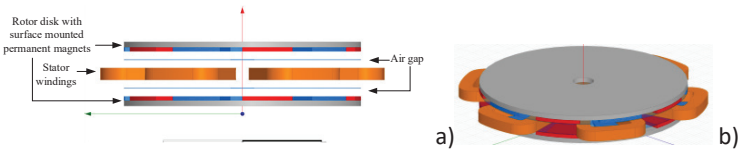

Figure 4: *Double-sided coreless AFPMM with two external rotors and one internal stator: a) components of the machine, b) model of the machine*

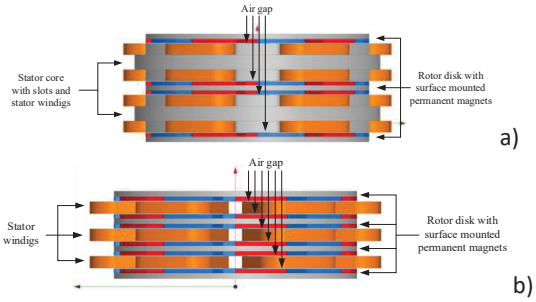

Figure 5: *Multistage AFPMM: a) with stator cores, b) coreless*

This article deals with the coreless double-sided topology with two outer rotor discs with surface-mounted permanent magnets and one inner coreless stator.

Since it is a coreless topology, there is no cogging torque present, *[16]*, and also no stator core losses. Due to the absence of the core losses, these types of generators can operate at higher efficiencies compared to conventional generators, *[2-5].*

These types of machines can be used for low-speed applications because they usually have a large pole number. Electromagnetic force (EMF) and torque production are mainly limited by:

- limited mass of the machine and its outer dimensions, due to the application of the machine, and
- limited electrical current density, due to the heating of the windings.

The outer dimensions of the machine limit the space for windings, and the permanent magnet (PM) installation and maximum allowed temperature limit the electrical current density in the windings *[7,18].*

EMF and torque depend on the magnetic flux density in the air gap, namely the axial component of the magnetic flux density in the air gap, which passes between PMs on opposite rotor disks, *[22].* This dependency is represented with Faraday's induction law for time changing magnetic field, *[36].*

Magnetic flux density in the air gap depends on:

- active copper volume, and *[19]*,
- PM volume (determined by PM thickness, pole number and inner and outer radius of the active part of the machine *[20]*) and
- electrical current density in the windings.

From the text above, it can be concluded that magnetic flux density in the air gap is one of the key values for torque and EMF production, since it is connected to all the machine dimensions and materials, *[23,24].*

Since this article deals with a coreless machine, a suitable stator thickness must be selected, because it also represents a large air gap for the magnetic flux density, *[26].* Suitable stator thickness reduces the magnetic flux leakage from the south to north pole on the same PM (Path 2 in Fig.6).

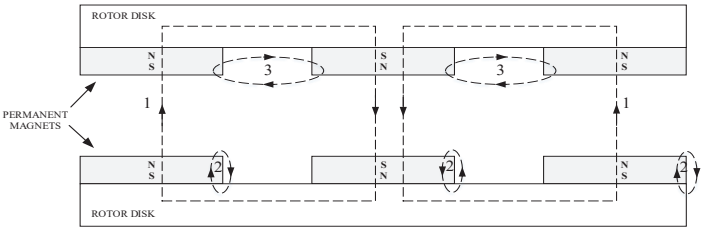

Figure 6: *Sectional view of AFPMM with magnetic flux paths*

Magnetic flux leakage between neighbouring PMs (Path 3 in Fig. 6) can be reduced with a suitable distance between them, *[27].* It must be considered that suitable stator thickness also influences the magnetic flux leakage presented as Path 3, and the angle of PMs influences the magnetic flux leakage presented with Path 2.

Many design methodologies for AFPMM are connected to simple design equations, *[20, 28, 29]*, used for preliminary design. Analytical methods offer a fast preview of torque production of the machine with a certain degree of accuracy, *[30].* The finite element method (FEM) is an accurate numerical method and requires much time for simulations, *[16, 20, 31-33, 35].* Recent works deal with solving this problem by developing different analytical methods, which require certain simplifications and assumptions, *[17]*, that influence the accuracy of the results but offer a faster determination of magnetic flux density in an explicit form, *[45].* Derivation of equations for magnetic flux density calculation from Maxwell's equations is a commonly used approach, *[35].*

This article presents a methodology for designing coreless AFPMM through using a polynomial for magnetic flux density calculation, which was determined by using the least square approximation (LSA) method.

Combining the polynomial and a well-known analytical equation for torque calculation, a new equation for the torque calculation of an AFPMM is determined for various stator thicknesses.

Torque was calculated for different stator thicknesses using the new equation and compared with the results of FEM analysis.

2 METHODOLOGY

2.1 Simplified FEM

The axial component of magnetic flux density in the middle of the stator was determined by a simplified finite element method (FEM) for different stator thicknesses of a double-sided coreless AFPMM.

The simplification of the FEM calculations is the use of the air between the rotor disks instead of the stator with its windings, which is possible due to the similarity of permeability of air and copper. The tool used was the Ansys Maxwell 3D software. The values of the axial component of the magnetic flux density in the middle of the stator (air) were obtained on a centreline between two permanent magnets for various stator thicknesses by using an LSA method, resulting in a polynomial for calculating the axial component of magnetic flux density in the middle of the stator for different stator thicknesses.

EMF and torque were calculated for different stator thicknesses and compared with the results of FEM analysis and measurements of the prototype machine.

A 3D model of the generator was constructed, which is based on an actual prototype, presented in *[36].* Its data are presented in Table 1. These dimensions were chosen for easier verification of the results with actual laboratory measurements.

Table 1: *Geometry and parameters of analysed AFPMM, [36]*

Symbol	Quantity	Value/Unit
R	Rotor disk radius	150 mm
d_{Fe}	Rotor disk thickness	7 mm
d_m	Permanent magnet thickness (NdFeB)	5 mm
τ_m	Magnetic pitch	25°
D_i	Inner diameter of PM	80 mm
D_o	Outer diameter of PM	150 mm
B_r	Remnant magnetic flux density	1.22 T
τ_p	Pole pitch	36 °
I	Electrical current	2x10 A
	Number of windings	6
d_s	Winding thickness	15 mm
d_c	Coil width	20 mm
S_w	Copper wire cross section	1.23 mm^2
d_{ag}	Air gap thickness	1 mm
m	Number of phases	3
k_w	Winding factor	0.966
p	Number of pole pairs	5

For different stator thicknesses, simplified FEM calculations were performed, based on which, the axial component of magnetic flux density was analysed on a centreline between the PMs on the opposite rotor disks. The position of the centreline and the dimensions of the PMs are shown in Fig. 7.

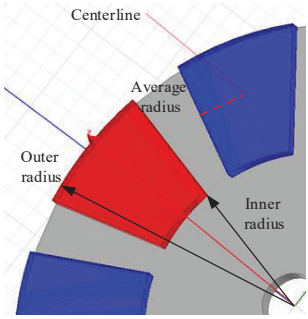

Figure 7: *Dimensions of the PMs and the centreline*

Fig. 8 shows the meshed model of rotor disks with surface mounted PMs with a 55 mm fictitious air gap between them, which represents the thickness of the stator and both air gaps.

The middle of the distance between PMs on the opposite rotor disks also represents the middle of the stator. Values of the axial component of the magnetic flux density were used to determine the polynomial for the calculation of magnetic flux density in the middle of the stator for different stator thicknesses.

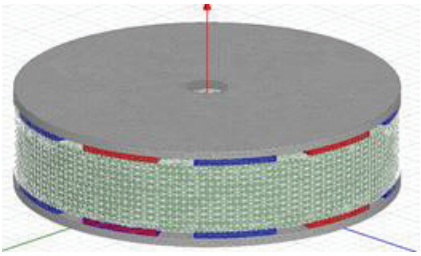

Figure 8: *Meshed AFPMM model with 55 mm fictitious air gap*

Fig. 9 shows a single value waveform for a 55 mm distance between PMs on opposite rotor disks (marked as a fictitious air gap) and the magnetic flux density values near the PM and in the middle of the stator, respectively marked as B_{z_max} and B_{z_min}.

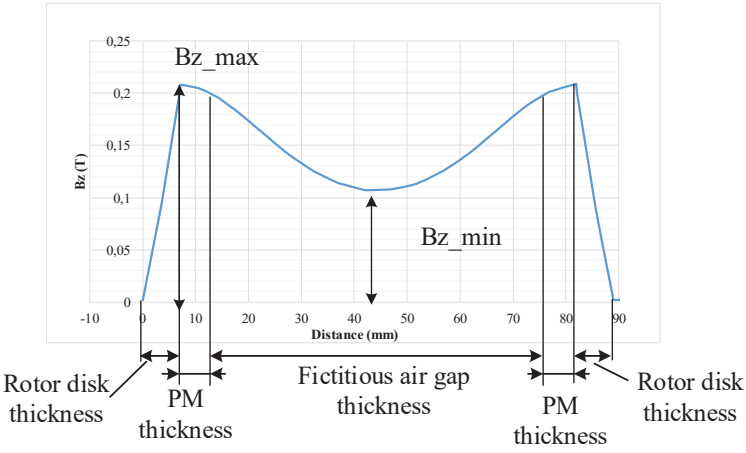

Figure 9: *Positions of maximum and minimum axial component magnetic flux density*

2.2 Least square approximation method

Values for B_{z_min} were used to produce a polynomial using an LSA method, which is a mathematical procedure that can find a curve that best fits a known set of given points by minimizing the sum of the squares of the offsets ("the residuals") of the points from the curve. The sum of the squares of the offsets is used instead of the absolute offset values because this allows the residuals to be treated as a continuous differentiable quantity, *[37].* Vertical least-squares fitting proceeds by finding the sum of the squares of the vertical deviations R^2 of a set of n data points, *[37]*, which is presented in (2.1).

$$R^2 \equiv \sum_{i=1}^{n} \left[y_i - f\left(x_i, a_1, a_2, \ldots, a_n\right) \right]^2 \tag{2.1}$$

.

where R is the residual, y_i FEM calculated data point, f fitting function, x_i independent variable of fitting function, a_1, a_2, and are coefficients of fitting function. In the present case the polynomial is chosen as a fitting function.

The condition for R^2 to be a minimum is that for i=1,…,n, the derivative of R^2 equals 0

$$\left(\frac{\partial R^2}{\partial a_i} = 0 \right).$$

As an example, if we use the linear fit (polynomial of fist order) $f(a,b)=a+bx$, we obtain the following set of equations (2.2), *[38].*

$$R^2(a,b) \equiv \sum_{i=1}^{n}\left[y_i - (a+bx_i)\right]^2$$
$$\frac{\partial(R^2)}{\partial a} = -2\sum_{i=1}^{n}\left[y_i - (a+bx_i)\right] = 0 \quad (2.2)$$
$$\frac{\partial(R^2)}{\partial b} = -2\sum_{i=1}^{n}\left[y_i - (a+bx_i)\right]x_i = 0$$

Using the procedure described above and a set of data points for B_{z_min}, a polynomial was determined. The analysis is carried out in the middle of the stator because the magnetic flux density is the lowest and presents the safe side in the design of the machine.

3 DESIGN OF AN AFPMG WITH LEAST SQUARE APPROXIMATION METHOD

The process of designing AFPMM machines as well as any other form of machine has steps, the first of which is defined by different limitations, such as required torque size, rotation speed, maximum allowed dimensions, etc. Therefore, the starting dimensions of the machine must be estimated with the highest possible accuracy, especially the inner and outer diameters of the PMs and axial length of the machine. A standard approach for determining these dimensions is the use of sizing equations, *[39, 40].*

Two types of sizing equations for AFPMM can be found in the literature. *[41].* Equation (3.1) includes (besides electrical and magnetic parameters) inner radius, outer radius and axial length of the machine, *[42].*

$$P_i = \eta \frac{m}{T}\int_0^T e(t)\,i(t)\,dt = \eta m K_p E_{pk} I_{pk} \quad (3.1)$$

where *i(t)* is phase electrical current, *m* number of phases, *e(t)* electromagnetic force (*EMF), η* efficiency of the machine, K_p electrical power waveform, *T* one period of EMF and E_{pk} and I_{pk} peak values of EMF and phase current [42].

This article deals with the second type of sizing equations, so the elements of (3.1) are not described in detail.

The second type of sizing equation (3.2) includes the connection between electromagnetic torque and basic geometrical, electrical and magnetic parameters.

$$T_{em} = \frac{\pi}{4} B_z A_{in} K_d \lambda \left(1-\lambda^2\right) D_o^3 \quad (3.2)$$

where T_{em} is the electromagnetic torque, A electrical current density and K_d flux leakage factor, λ ratio between the inner and outer diameter of the PMs, D_o outer diameter of the PM *[44]*. Considering the line current density, Equation (3.2) can be written as (3.3)

$$T_{em} = \frac{1}{4}\alpha_i mINk_w B_z \left(D_o^2 - D_i^2\right) \tag{3.3}$$

where α_i is the angle of PMs divided by the pole angle, m number of phases, I electrical current, k_w winging factor, N number of turns per coil, B_z axial component of magnetic flux density and D_o and D_i outer and inner PM diameter respectively.

By inserting the polynomial for determining the axial component of magnetic flux density in the middle of the fictitious air gap into equation (3.3), a new equation emerges for electromagnetic torque calculation that considers different stator thicknesses.

4 RESULTS

Simplified FEM was used to produce a set of data points for B_{z_min} and B_{z_min} for the AFPMM described in Table 1. Fig. 10 and Table 2 show that the maximum and minimum values of B_z are very close up to the 25mm fictitious air gap thickness.

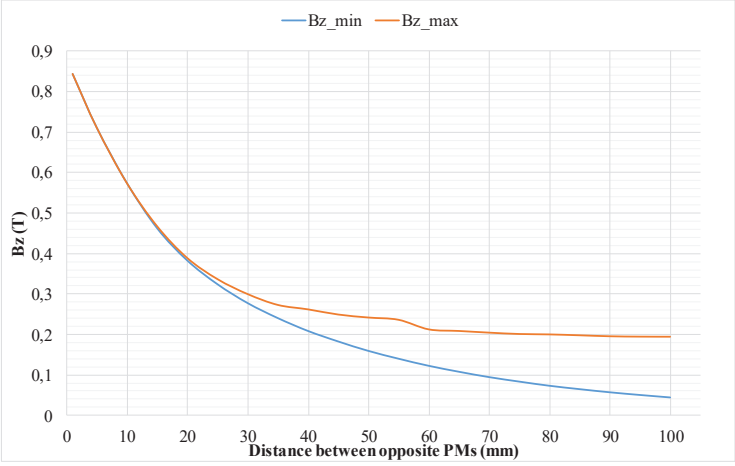

Figure 10: *Bz_max and Bz_min in axial direction between the PMs*

Table 2: *Axial component of magnetic flux density in the fictitious air gap (simplified FEM)*

Distance between opposite PMs d (mm)	B_{z_min} (T)	B_{z_max} (T)	Difference (%)
1	0.8448	0.8448	0
5	0.7118	0.7118	0
10	0.5745	0.5745	0
15	0.4628	0.4682	1.15
20	0.3828	0.3895	1.71
25	0.3241	0.3373	3.94

Using the LSA and data from Table 2, a polynomial (4.1) was determined for the axial component of magnetic flux density in the middle of the stator for different stator thicknesses.

$$B_z = 0,883941142648657 - 0,038685876107852 \cdot d + 0,000823824267761 \cdot d^2 - 0,000006968242777 \cdot d^3 \quad (4.1)$$

where B_z is the axial component of magnetic flux density in the middle of the fictitious air gap and d the thickness of the fictitious air gap. By inserting (4.1) into (3.3), a new equation (4.2) emerges for electromagnetic torque calculation that considers different stator thicknesses.

$$T_{em} = \frac{1}{4}\alpha_i mINk_w \begin{pmatrix} 0,8839 - \\ 0,0387 \cdot d + \\ 0,8238 \cdot 10^{-3} \cdot d^2 - \\ 0,6968 \cdot 10^{-5} \cdot d^3 \end{pmatrix} \left(D_o^2 - D_i^2\right) \quad (4.2)$$

We have derived a new polynomial for calculating the axial component of magnetic flux density in the middle of the stator for different stator thicknesses for the maximum of 25 mm stator thickness together with air gaps on both sides, because the results in Table 2 show the acceptable deviation of 3.94% at fictitious air gap 25 mm.

4.1 Verification of results

Equation (4.2) represents a new equation for AFPMM electromagnetic torque calculation for optimal stator thicknesses. Verification of the electromagnetic torque calculation is performed by comparing the calculated results, gained by using equation (4.2), and the results gained by FEM simulations of the AFPMM described in Table 1.

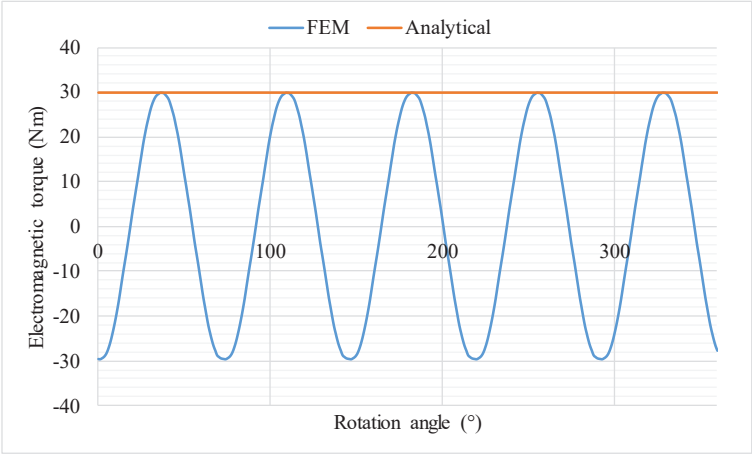

Figure 11: *Comparison of FEM and analytically calculated electromagnetic torque*

Fig. 11 shows the calculated electromechanical (static) torque gained by using equation (4.2) and FEM. The result gained by equation (7) is 29.82 Nm and 29.78 Nm by FEM, which means that there is only 0.15% difference.

FEM and analytically calculated results are also compared to the results of measurements of the actual prototype. Measurement results are reported in *[43]*, and for 600 rpm rotational speed electromechanical torque of 29.4 Nm was measured. Calculated results are in good agreement with the measured value: the difference between them is less than 1.5%.

Additional FEM analysis were performed for 3 stator thicknesses (5, 10, and 20 mm). Fig. 12 shows the comparison of results.

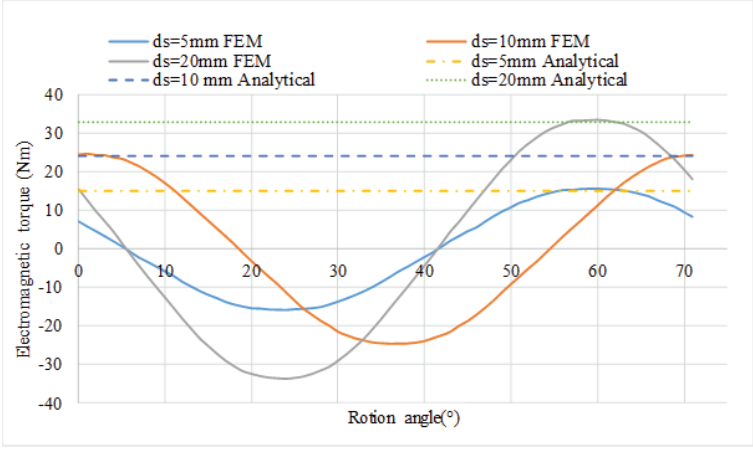

Figure 12: *Comparison of FEM and analytically calculated electromagnetic torque for different stator thicknesses*

Matching between the FEM and analytically calculated torque for 5 mm stator thickness is 96.5%, 98.06% for 10 mm stator thickness, and 98.34% for 20 mm stator thickness

5 CONCLUSION

This article presents a methodology for designing AFPMM, especially in the preliminary stage. Once the initial geometrical parameters are determined, a few simplified FEM calculations combined with LSA can produce a polynomial that offers a fast preview of the EMF and torque production of the machine for different stator thicknesses. Agreement between the results obtained via FEM, the analytically calculated results, and measured results for one stator thickness confirms that the presented methodology offers quite accurate results.

References

[1] **F. Danang Wijaya, N. A. Rahadyan, and H. R. Ali**, "Magnetic flux distribution due to the effect of stator-rotor configuration in the axial machine," Proc. - 2014 6th Int. Conf. Inf. Technol. Electr. Eng. Leveraging Res. Technol. Through Univ. Collab. ICITEE 2014, no. d, 2015.

[2] **S. Ekram**, "A novel windmill generator," Proc. - 12th Int. Conf. Electr. Mach. Syst. ICEMS 2009, 2009.

[3] **A. Pop, F. Gillon, and M. M. Radulescu**, "Modeling and permanent-magnet shape optimization of an axial-flux machine," Proc. - 2012 20th Int. Conf. Electr. Mach. ICEM 2012, no. c, pp. 357–363, 2012.

[4] **Y. Cao, L. Yu and H. Jia**, "Rotor mechanical stress and deformation analysis of coreless stator axial-flux permanent magnet machines," *2015 IEEE Magnetics Conference (INTERMAG)*, Beijing, 2015, pp. 1-1.

[5] **X. Wei and K. Yang**, "Research of stator displacement technique in multi-stage axial-flux permanent magnet machines," *2015 IEEE Magnetics Conference (INTERMAG)*, Beijing, 2015, pp. 1-1.

[6] **F. Caricchi, F. Crescimbini, F. Mezzetti, and E. Santini**, "Multi-stage axial-flux pm machine for wheel direct drive," IEEE Trans. Ind. Appl., vol. 32, no. 4, pp. 882–888, 1996.

[7] **A. Daghigh, H. Javadi and H. Torkaman**, "Improved design of coreless axial flux permanent magnet synchronous generator with low active material cost," *The 6th Power Electronics, Drive Systems & Technologies Conference (PEDSTC2015)*, Tehran, 2015, pp. 532-537.

[8] **L. Drazikowski and W. Koczara**, "Permanent magnet disk generator with coreless windings," COMPEL Int. J. Comput. Math. Electr. Electron. Eng., vol. 31, no. 1, pp. 108–118, 2012.

[9] **A. Hemeida, P. Sergeant, A. Rasekh, H. Vansompel and J. Vierendeels**, "An optimal design of a 5MW AFPMSM for wind turbine applications using analytical model," *2016 XXII International Conference on Electrical Machines (ICEM)*, Lausanne, 2016, pp. 1290-1297.

[10] **M. Aydin, M. Gulec, Y. Demir, B. Akyuz, and E. Yolacan**, "Design and validation of a 24-pole coreless axial flux permanent magnet motor for a solar powered vehicle," 2016 XXII Int. Conf. Electr. Mach., pp. 1493–1498, 2016.

[11] **N. Takorabet, J. P. Martin, F. Meibody-Tabar**, F. Sharif, and P. Fontaine, "Design and optimization of a permanent magnet axial flux wheel motors for electric vehicle," Proc. - 2012 20th Int. Conf. Electr. Mach. ICEM 2012, no. c, pp. 2635–2640, 2012.

[12] **R.-B. Mignot, F. Dubas, C. Espanet, and E. D. Chamagne**, "Design of axial flux PM motor for electric vehicle via a magnetic equivalent circuit," 2012 First Int. Conf. Renew. Energies Veh. Technol., pp. 212–217, 2012.

[13] **N. Takorabet, J. P. Martin, F. Meibody-Tabar, F. Sharif and P. Fontaine**, "Design and optimization of a permanent magnet axial flux wheel motors for electric vehicle," *2012 XXth International Conference on Electrical Machines*, Marseille, 2012, pp. 2635-2640.

[14] **T.-U. Jung**, "Electromagnetic design analysis and performance improvement of axial field permanent magnet generator for small wind turbine," J. Appl. Phys., vol. 111, no. 7, p. 07E708, 2012.

[15] **G. J. Yan, L. Y. Hsu, J. H. Wang, M. C. Tsai, and X. Y. Wu**, "Axial-flux permanent magnet brushless motor for slim vortex pumps," IEEE Trans. Magn., vol. 45, no. 10, pp. 4732–4735, 2009.

[16] **F. Giulii Capponi, G. De Donato, and F. Caricchi**, "Recent advances in axial-flux permanent-magnet machine technology," IEEE Trans. Ind. Appl., vol. 48, no. 6, pp. 2190–2205, 2012.

[17] **Z. Shabahang, M. Shahnazari and A. Sedighi**, "Analysis of dynamic eccentricity in a coreless axial flux permanent magnet machine," *2015 30th International Power System Conference (PSC)*, Tehran, 2015, pp. 358-362.

[18] **Chen, R. Nilssen, and A. Nysveen**, "Performance comparisons among radial flux, multi-stage axial flux and three-phase transverse flux pm machines for downhole applications," 2009 IEEE Int. Electr. Mach. Drives Conf. IEMDC '09, pp. 1010–1017, 2009.

[19] **Hanselman, D.**: Brushless permanent magnet motor design, Magna Physics Pub., USA, 2006.

[20] **Gieras, J.F., Wang, R.J., Kamper M.J.**, Axial Flux Permanent Magnet Brushless Machines, Kluwer Academic Publishers, Dordrecht, 2004.

[21] **S. Lomheim**, "Analysis of a Novel Coil Design for Axial Flux Machines," M.S. Thesis, Norwegian University of Science and Technology, Department of Electric Power Engineering, Jun. 2013.

[22] **W. Jara, A. Martin, and J. A. Tapia**, "Axial flux PM machine for low wind power generation," 19th Int. Conf. Electr. Mach. ICEM 2010, 2010.

[23] **Daghigh, H. Javadi, and A. Javadi**, "Improved Analytical Modeling of Permanent Magnet Leakage Flux in Design of the Coreless Axial Flux Permanent Magnet Generatorx," Can. J. Electr. Comput. Eng., vol. 40, no. 1, pp. 3–11, 2017.

[24] **Caricchi, F. Crescimbini, O. Honorzti, G. Lo Bianco and E. Santini**, "Performance of coreless-winding axial-flux permanent-magnet generator with power output at 400 Hz-3000 rev/min," *Industry Applications Conference, 1997. Thirty-Second IAS Annual Meeting, IAS' 97., Conference Record of the 1997 IEEE*, New Orleans, LA, 1997, pp. 61-66 vol.1.

[25] **M. Sadeghierad, H. Lesani, H. Monsef and A. Darabi**, "Leakage flux consideration in modeling of high speed axial flux PM generator," *2008 IEEE International Conference on Industrial Technology*, Chengdu, 2008, pp. 1-6.

[26] **Lee, K. Jeon, Y. Kim and S. Jung**, "Performance evaluation of coreless axial flux permanent magnet wind generator," *2015 IEEE Magnetics Conference (INTERMAG)*, Beijing, 2015, pp. 1-1.

[27] **Mbidi, David Natangue**, "Design and Evaluation of a 300 kW Double Stage Axial-Flux Permanent Magnet Generator," M.S. Thesis, Stellenbosch University, 2001.

[28] **S. Kahourzade, A. Mahmoudi, N. A. Rahim, and H. W. Ping**, "Sizing equation and finite element analysis optimum design of axial-flux permanent-magnet motor for electric vehicle direct drive," 2012 IEEE Int. Power Eng. Optim. Conf. PEOCO 2012 - Conf. Proc., no. June, pp. 1–6, 2012.

[29] **V. Rallabandi, N. Taran, D. M. Ionel, and J. F. Eastham**, "On the feasibility of carbon nanotube windings for electrical machines - Case study for a coreless axial flux motor," ECCE 2016 - IEEE Energy Convers. Congr. Expo. Proc., 2017.

[30] **Y. Wang, W. X. C. Chen, and Z. Dong**, "A parametric magnetic network model for axial flux permanent magnet machine with coreless stator," 2014 17th Int. Conf. Electr. Mach. Syst. ICEMS 2014, pp. 1108–1113, 2015.

[31] **J. M. Seo, I. S. Jung, H. K. Jung and J. S. Ro**, "Analysis of Overhang Effect for a Surface-Mounted Permanent Magnet Machine Using a Lumped Magnetic Circuit Model," in *IEEE Transactions on Magnetics*, vol. 50, no. 5, pp. 1-7, May 2014.

[32] **A. Mahmoudi, N. a. Rahim, and W. P. Hew**, "Axial-flux permanent-magnet machine modeling, design, simulation and analysis," Sci. Res. Essays, vol. 6, no. 12, pp. 2525–2549, 2011.

[33] **N. Taran and M. Ardebili**, "A novel approach for efficiency and power density optimization of an Axial Flux Permanent Magnet generator through genetic algorithm and finite element analysis," *2014 IEEE 23rd International Symposium on Industrial Electronics (ISIE)*, Istanbul, 2014, pp. 709-714.

[34] **J. Azzouzi, G. Barakat, and B. Dakyo**, "Quasi-3D analytical modeling of the magnetic field of an axial flux permanent magnet synchronous machine," Electr. Mach. Drives Conf. 2003. IEMDC'03. IEEE Int., vol. 3, no. 4, pp. 1941–1947 vol.3, 2003.

[35] **P. Virtic, P. Pisek, T. Marcic, M. Hadziselimovic and B. Stumberger,** "Analytical Analysis of Magnetic Field and Back Electromotive Force Calculation of an Axial-Flux Permanent Magnet Synchronous Generator With Coreless Stator," in *IEEE Transactions on Magnetics*, vol. 44, no. 11, pp. 4333-4336, Nov. 2008.

[36] **P. Virtič, M. Vražić and G. Papa,** "Design of an Axial Flux Permanent Magnet Synchronous Machine Using Analytical Method and Evolutionary Optimization," in *IEEE Transactions on Energy Conversion*, vol. 31, no. 1, pp. 150-158, March 2016.

[37] **Weisstein, Eric W.** "Least Squares Fitting." From MathWorld--A Wolfram Web Resource. http://mathworld.wolfram.com/LeastSquaresFitting.html

[38] **Kenney, J. F. and Keeping, E. S.** "Linear Regression and Correlation." Ch. 15 in Mathematics of Statistics, Pt. 1, 3rd ed. Princeton, NJ: Van Nostrand, pp. 252-285, 1962.

[39] **A. Chen, R. Nilssen, and A. Nysveen**, "Performance comparisons among radial-flux, multi-stage axial-flux, and three-phase transverse-flux PM machines for downhole applications," IEEE Trans. Ind. Appl., vol. 46, no. 2, pp. 779–789, Apr. 2010.

[40] **O. Kalender, Y. Ege, and S. Nazlibilek**, "Design and determination of stator geometry for axial flux permanent magnet free rod rotor synchronous motor," Measurement, vol. 44, no. 9, pp. 1753–1760, 2011.

[41] **J. Pyrhönen, T. Jokinen, and V. Hrabovcová**, Design of Rotating Machines, Chichester, U.K.: Wiley, 2009.

[42] **S. Huang, J. L. F. Leonardi, and T. A. Lipo**, "A comparison of power density for axial flux machines based on general purpose sizing equations," IEEE Trans. Energy Convers., vol. 14, no. 2, pp. 185–192, Jun. 1999.

[43] **P. Virtič**, "Načrtovanje in analiza sinhronskih strojev s trajnimi magneti in aksialnim magnetnim pretokom," Doctoral thesis, University of Maribor, Maribor, 2008.

[44] **E. Spooner and B. J. Chalmers**, ""TORUS": A slotless, toroidal-stator, permanent-magnet generator," Proc. Inst. Elect. Eng.—Elect. Power Appl., vol. 139, no. 6, pp. 497–506, Nov. 1992.

Nomenclature

(Symbols)	(Symbol meaning)
R	rotor disk radius
d_{Fe}	rotor disk thickness
d_M	permanent magnet thickness
τ_m	magnetic pitch
D_i	inner radius of PM
D_o	outer radius of PM
B_r	remnant magnetic flux density
τ_p	pole pitch
p	number of pole pairs
I	rated phase current
$i(t)$	phase electrical current,
$e(t)$	electromagnetic force
η	efficiency of the machine
K_p	electrical power waveform
K_d	flux leakage factor

T	one period of EMF
E_{pk}	peak value of EMF
I_{pk}	peak value of phase current
B_{z_max}	magnetic flux density near the PM
B_{z_min}	magnetic flux density in the middle of the stator
R	Residual in LSA
y_i	FEM calculated data point
f	fitting function
x_i	independent variable of fitting function
a_1, a_2	fitting function coefficients
A	electrical current density
T_{em}	electromagnetic torque
λ	ratio between inner and outer diameter of the PMs
α_i	angle of PMs divided with the pole angle
B_z	axial component of magnetic flux density
d	thickness of the fictitious air gap
N	number of turns per coil
d_c	coil width
d_s	stator thickness
m	number of phases
d_{ag}	air-gap thickness
S_W	Copper wire cross-section
k_w	winding factor